Journal of the Korean Society for Nondestructive Testing
Vol. 30, No. 6 (2010. 12)

Finite Element Analysis of Harmonics Generation by Nonlinear Inclusion

Seung-Yong Yang*† and Nohyu Kim**

Abstract When ultrasound propagates to a crack, transmitted and reflected waves are generated. These waves have useful information for the detection of the crack lying in a structure. When a crack is under residual stress, crack surfaces will contact each other and a closed crack is formed. For closed cracks, the fundamental component of the reflected and transmitted waves will be weak, and as such it is not easy to detect them. In this case, higher harmonic components will be useful. In this paper, nonlinear characteristic of a closed crack is modeled by a continuum material having a tensile-compressive unsymmetry, and the amplitude of the second harmonic wave was obtained by spectrum analysis. Variation of the second harmonic component depending on the nonlinearity of the inclusion was investigated. Two-dimensional plane strain model is considered, and finite element software ABAQUS/Explicit is used.

Keywords: Closed Crack, Finite Element Modeling, Ultrasound, Harmonics

1. Introduction

Nondestructive tests using ultrasound are being used widely to detect the size and location of cracks. However, when cracks are closed tightly by compressive residual stress, they do not produce linear scattering waves during reflection/transmission of ultrasound. Contact-type discontinuity such as closed cracks leads to an anomalously high level of nonlinearity. Well-known acoustical manifestation of the nonlinear behavior is the generation of its harmonics. Usefulness of nonlinear ultrasound effect has been studied by Ha and Jhang (2006).

The physical nature of the contact acoustic nonlinearity(CAN) has been explained by developing several mathematical models of contact-type interface (Biwa et al., 2005 and 2007; Kim et al., 2004; Roy and Pyrak-Nolte, 1995). From their works, the variation of contact area due to deformation of asperities is known to cause nonlinear elasticity of the interface. This interface is considered as a linear spring whose stiffness is proportional to the contact area within the interface. The spring-type crack interface connects displacement discontinuity across the interface with the traction on both sides. Due to the nonlinear nature of the contacting discontinuity, the stress-strain curve is unsymmetric and higher order harmonics can be generated for reflected or transmitted waves (see Fig. 1).

In this paper, fundamental and higher harmonic components of reflected waves by nonlinear inclusions are calculated. A nonsymmetric material having different elastic moduli for tensile and compressive states is considered to account for the nonlinearity of

Received: November 4, 2010. Revised: December 6, 2010. Accepted: December 10, 2010. *Department of Mechatronic Engineering, Korea University of Technology, 307 Gajun-Ri, Byungchun-Myun, Chunan 330-860, Korea, **Department of Mechanical Engineering, Korea University of Technology and Education, 307 Gajun-Ri, Byungchun-Myun, Chunan 330-860, Korea, †Corresponding Author: ysy@kut.ac.kr

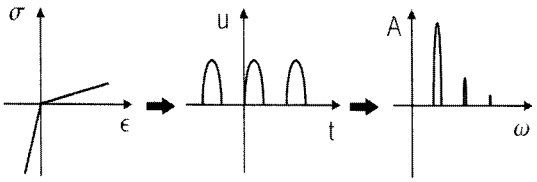

Fig. 1 Nonlinear response of contact-type discontinuity and the harmonics generation

closed cracks. 2-dimensional plane strain finite element model having a very thin layer of the unsymmetric nonlinear material at the center was considered. Stress wave propagation of incident ultrasonic wave was solved by finite element code ABAQUS/Explicit (ABAQUS, 2006). The harmonic components were obtained by the fast Fourier transformation algorithm of numerical recipes (Press et al., 1988).

2. Finite Element Model

Fig. 2 shows two-dimensional finite element model with a 15 degree-inclined layer of nonlinear material at the center and the displacement input on the left. The inclination angles of 0 degree and 15 degree were considered in this paper. The inclusion is 20 mm long and 0.1 mm thick. It is modeled by one row of 200 quadrilateral finite elements each of which is 0.1 mm×0.1 mm. Vertical displacement is set zero on the upper and lower boundaries of the model. Fig. 3 shows a magnified view of the finite element mesh used in the calculation.

The embedded inhomogeneity physically means a nonlinear closed crack. A typical anomalous behavior of a closed crack is that the traction vs. displacement behavior can be different for tension and compression. This unsymmetric behavior can be incorporated by at least two methods. One is using cohesive zone interface elements and the other is employing a thin layer of continuum elements. The former needs a traction-displacement constitutive relation and the latter should be described by a stress vs. strain relation. The continuum element

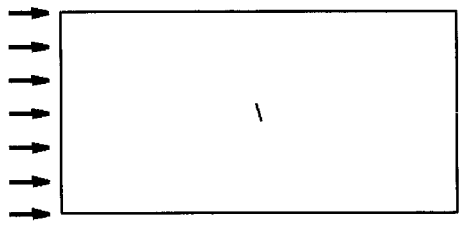

Fig. 2 Plane strain model with 15 degree-inclined inclusion

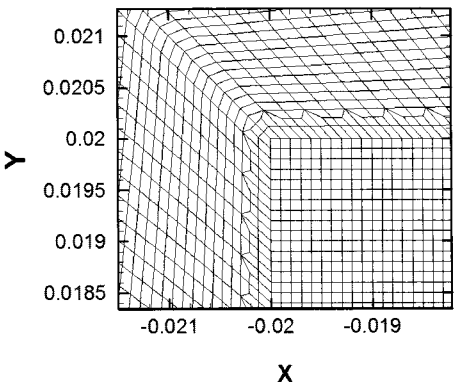

Fig. 3 Details of the finite element mesh

approach is used in this paper to account for the contact-type discontinuity.

To descibe the constitutive equation of the inclusion, user material subroutine VUMAT was used. The elastic modulus will be different depending on the normal strain component ϵ_{nn} given by the following equation

$$\epsilon_{nn} = n \cdot \epsilon n \tag{1}$$

where n is the unit normal vector to the discontinuity surface. The following unsymmetric Young's modulus was used assuming isotropic material behavior.

$$\begin{aligned} E &= E_1 \quad \text{for} \quad \epsilon_{nn} < 0 \\ E &= E_2 \quad \text{for} \quad \epsilon_{nn} \geqq 0 \end{aligned} \tag{2}$$

Poisson's ratio is the same for either case. Young's modulus and Poisson's ratio for the surrounding matrix are 200 GPa and 0.3, respectively.

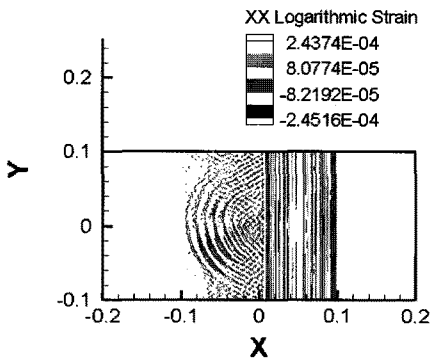

Fig. 4 Example of contour plot of ϵ_{xx} for toneburst incident wave

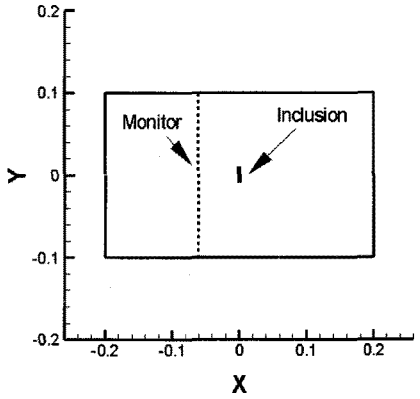

Fig. 6 Position of the monitoring nodal points

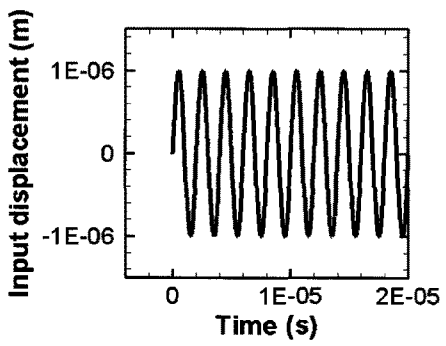

Fig. 5 Harmonic incident wave of displacement u_x

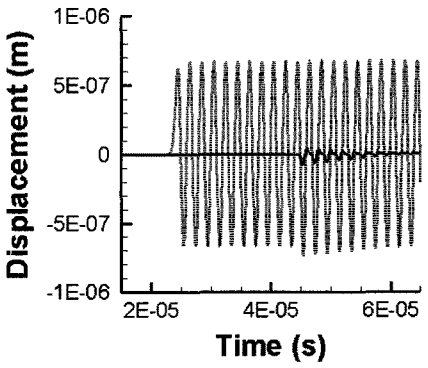

Fig. 7 Horizontal displacement u_{crack} (dotted line) and $u_{scatter}$ (solid line) at a point

Fig. 4 shows a typical calculation result. One can see that the reflected wave is superimposed on the incident toneburst wave in the contour plot.

3. Fourier Transformation

Fig. 5 shows the profile of the incident harmonic displacement wave applied on the left boundary of the model. The frequency is 500,000 Hz.

The reflected wave was monitored at the nodal points depicted in Fig. 6. The scattered wave by the inclusion can be obtained by subtracting two displacement results: one is with the inclusion, and the other without the inclusion.

$$u_{scatter} = u_{crack} - u_{nocrack} \tag{3}$$

To obtain results without the inclusion, finite element calculation was carried out separately for the homogeneous body. Fig. 7 shows the displacements at the center of the monitoring line for the input of harmonic wave. u_{crack} is denoted by the dotted line and $u_{scatter}$ is the solid line calculated by (3). The incident wave arrives at the point about 20 micro second and the reflected wave is obsolved at 45 micro second.

Fourier transformation of the scattered waves was calculated by twofft subroutine of Numerical recipes. twofft computes Fourier transformation of real valued data. A typical frequency spectrum result is shown in Fig. 8. Harmonics are observed around at the multiples of the fundamental frequency, 500 kHz.

Table 1 Material parameters

	$\theta=0^\circ$	$\theta=15^\circ$
E_1	$200GPa$	$200GPa$
E_2	$7GPa$ $10GPa$ $20GPa$ $30GPa$ $50GPa$	$20GPa$
ν	0.3	0.3

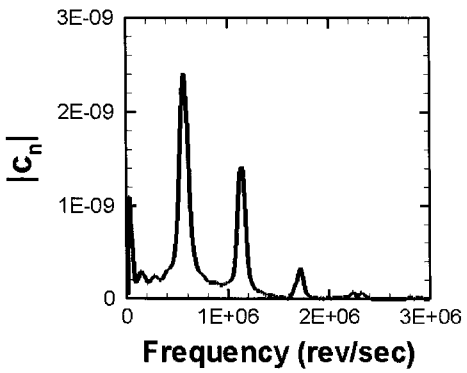

Fig. 8 Example of Fourier transformation result

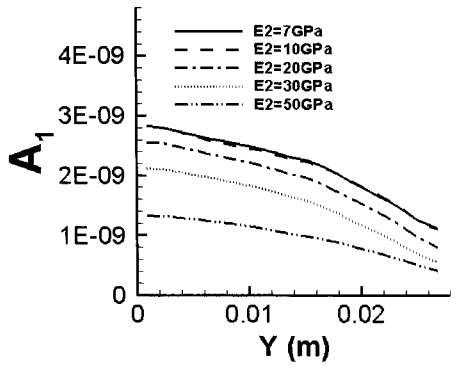

Fig. 9 Amplitude of fundamental frequency component, A_1. $\theta=0^\circ$ is used

The analysis was carried out for various values of E_1 and E_2 listed in Table 1. That is, for each case of Table 1, finite element calculation was carried out, and the magnitude of the displacement of the scattered wave was obtained at the monitoring points. Fourier transformation was conducted for the signal.

Fig. 9 shows the amplitude of the fundamental component (peak value around 500,000 Hz) of the scattered waves. The value

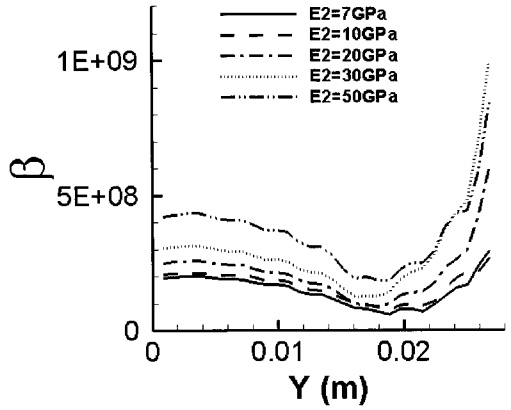

Fig. 10 Ratios of second harmonic to first harmonic, $\beta=A_2/A_1^2$. $\theta=0^\circ$ is used

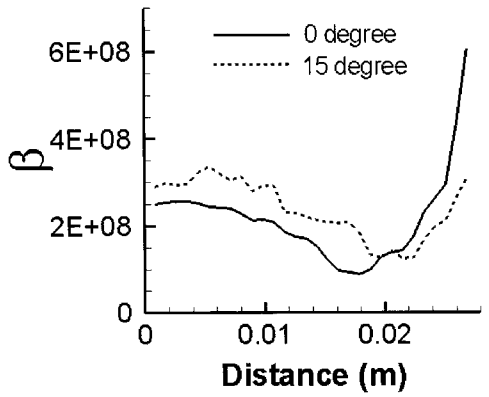

Fig. 11 Ratios of second harmonic to first harmonic $\beta=A_2/A_1^2$ for different oblique angles θ

decreases as the tensile Young's modulus approaches the compressive one. That is, as the nonlinear effect is small, the scattered signal will be weak, as anticipated. The values on the abscissa mean the distance from the center of the monitoring line. The value of A_1 decreases as moving away from the center of the reflected wave.

Fig. 10 shows a ratio of the second harmonic component to the fundamental component, given by a nonlinear parameter $\beta=A_2/A_1^2$ in Choi et al., (2002) For the perpendicular inclusion to the incident wave ($\theta=0^\circ$ case), the relative magnitude of the second harmonic component increases as the

value of E_2 approaches E_1, or in other words the scattered wave becomes weak. This result suggests that using the second harmonic component should be effective for detecting an inclusion such as a closed crack.

Fig. 11 shows the value of β for the cases of $\theta = 0^\circ$ and $\theta = 15^\circ$. The overall trends are similar. $E_1 = 200\,GPa$ and $E_2 = 20\,GPa$ were used for both.

4. Conclusions

Finite element calculation was carried out for a plate with a nonlinear elastic inclusion which has unsymmetric stress-strain behavior for tension and compression. From frequency spectrum analysis of the scattered wave it is observed that:

1. The scattered wave has strong higher order harmonic components
2. As the fundamental frequency component becomes weak, the ratio of the second harmonic to first harmonic components, $\beta = A_2/A_1^2$, increases.

Acknowledgment

This work was supported by the Korea Science and Engineering Foundation (KOSEF) grant funded by the Korea government (MEST) (No. 2007-00467)

References

ABAQUS (2006) Users Manual V. 6.6.1, HKS Inc.

Biwa, S., Suzuki, A. and Ohno, N. (2005) Evaluation of Interface Wave Velocity, Reflection Coefficients and Interfacial Stiffness of Contacting Surfaces, *Ultrasonics*, Vol. 43, pp. 495-502

Biwa, S., Hiraiwa, S., Matsumoto, E. (2007) Stiffness Evaluation of Contacting Surfaces by Bulk and Interface Waves, *Ultrasonics*, Vol. 47, pp. 123-129

Choi, Y. H., Kim, H. M., Jhang, K. Y. and Park, I. K. (2002) Application of Non-Linear Acoustic Effect for Evaluation of Degradation of 2.25Cr-1Mo Steel, *Journal of the Korean Society for Nondestructive Testing*, Vol. 22, pp. 170-176

Ha, J. and Jhang, K-Y. (2006) Detection and Imaging Processing of Interfacial Micro-Delamination in the Thin-Layered Structure by Using Nonlinear Ultrasonic Effect, *Key Engineering Materials*, Vol. 321-323, pp. 1513-1516

Kim, J.-Y., Baltazar, A., Rokhlin, S. I. (2004) Ultrasonic Assessment of Rough Surface Contact between Solids from Elastoplastic Loading-Unloading Hysteresis Cycle, *Journal of the Mechanics and Physics of Solids*, Vol. 52, pp. 1911-1934

Press, W. H,. Flannery, B. P., Teukolsky, S. A. and Vetterling, W. T. (1988) *Numerical Recipes in C*, Cambridge University Press, pp 407-424

Roy, S. and Pyrak-Nolte, L. J. (1995) Interface Waves Propagating along Tensile Fractures in Dolomite, *Geophys. Res. Lett.* Vol. 22 (2), pp. 2773-2776